Mapping Atomic Motions with Ultrabright Electrons: The Chemists' Gedanken Experiment Enters the Lab Frame

R.J. Dwayne Miller

Max Planck Institute for the Structure and Dynamics of Matter, Hamburg 22761, Germany, and Departments of Chemistry and Physics, University of Toronto, Toronto, Ontario M5S 3H6, Canada; email: dwayne.miller@mpsd.mpg.de

Annu. Rev. Phys. Chem. 2014. 65:583–604

First published online as a Review in Advance on January 9, 2014

The *Annual Review of Physical Chemistry* is online at physchem.annualreviews.org

This article's doi: 10.1146/annurev-physchem-040412-110117

Keywords

atomically resolved reaction dynamics, structure-function correlation of biological systems, femtosecond electron diffraction, high-brightness electron source development, mode coupling in transition state regions, nanofluidics for electron probes

Abstract

This review documents the development of high–bunch charge electron pulses with sufficient combined spatiotemporal resolution and intensity to literally light up atomic motions. This development holds promise in coming to a first-principles understanding of diverse problems, ranging from molecular reaction dynamics and structure-function correlations in biology to cooperativity in strongly correlated electron-lattice systems. It is now possible to directly observe the key modes involved in propagating structural changes and the enormous reduction in dimensionality that occurs in barrier crossing regions, which is central to chemistry and makes reaction mechanisms transferrable concepts. This information will help direct theoretical advances that will undoubtedly lead to generalized principles with respect to scaling relations in structural dynamics that will bridge chemistry to biology. In this quest, the limitations and future directions for further development are discussed to give an overview of the present status of the field.

1. INTRODUCTION

One of the long-standing goals in chemistry is to watch atoms move in real time—to directly observe the primary events governing chemical processes. This objective requires, in concert, subangstrom spatial resolution, subpicosecond time resolution, and sufficient intensity to collectively reach sufficient brightness to literally light up atomic motions. This objective has been met (1–5). We are presently at a major turning point in our ability to atomically resolve structural dynamics that is akin to the early days of the exploitation of X-ray and electron sources to give us our first atomically resolved static structures.

To get some sense of the promise that lies ahead for this emerging field of atomically resolved dynamics, imagine being able to watch the nuclear motions through a barrier crossing event. Such a direct observation captures the key modes involved in propagating the system through the transition state region—a central concept in chemistry (6–9). Similarly, biological functions are powered by chemical processes in which the protein structure has been evolutionarily optimized to control barrier crossing. In this context, static structures are insufficient. There is now an opportunity to directly resolve the structure-function correlation of biological systems to understand how these highly evolved structures direct chemical processes. In this respect, there are inherent correlation length scales and timescales in how proteins coarse-grain sample their potential energy surface (10–16). From optical measurements, the inherent collective modes of proteins have been shown to be involved, in which the reaction coordinate of the protein must be treated globally (11, 15, 17–21). One can make qualitative arguments about important structural features in proteins, but it is essential to directly observe the functional response of proteins at an atomic level to cast out the topological connection to functionally relevant motions. This objective has been the main driving force for my group's research efforts in the development of ultrabright electron sources (21). We are getting close.

The primary event of interest is the nuclear sampling of a critical point or transition state (the point of no return) that defines the barrier separating the reactant and product channels (6). As chemists, we are taught to visualize the relative atomic motions involved in these barrier crossing events as part of the mechanism-building process to better understand and direct chemistry along preferred pathways, to control chemistry. I define this to be the chemists' gedanken experiment. It is this thought process that binds the different disciplines of chemistry together and provides a common language. With the advent of ultrabright electron (1, 2, 4, 22) and X-ray sources (5, 23, 24), as well as recent developments with laser plasma sources for X-ray powder diffraction (25, 26), we can now directly watch atomic motions to bring this classic thought experiment into direct experimental observation.

2. DIRECT OBSERVATION OF THE REDUCTION IN DIMENSIONALITY DURING BARRIER CROSSING

In terms of advancing the conceptual basis for chemistry, the most important development to come from this emerging field is to provide a direct observation of the far-from-equilibrium motions involved in barrier crossing. In this respect, there has been an interesting sleight of hand done in conventional pedagogical approaches to teaching chemistry. On the one hand, students are faced with memorizing a large number of standard reaction mechanisms to develop skills in designing synthetic strategies, whereas on the other hand, transition state theory teaches the importance of nuclear fluctuations or modes sampling critical points that intersect reactant and product surfaces. This dichotomy in the teaching of chemistry is worth considering. Each molecule should have different modal character in sampling barrier regions and should behave differently.

How is it then possible for chemistry to involve transferrable concepts such as classes of reaction mechanisms? Moreover, there are so many possible arrangements of the constituent atoms in any given molecular system of interest that it is remarkable that we can find predictable trends to reactions at all. For example, for a reaction involving N atoms, of the order of $3N$ dimensions are needed to describe all possible nuclear motions in a chemical process. For typical problems of interest, the total number of possible nuclear permutations approaches astronomical proportions. Creating a $3N$ dimensional potential energy surface to describe nuclear motions for systems of interest (beyond three atoms) is not practical and does not capture the dominant terms in the many-body potential that leads the system through a chemical passage. The magic of chemistry is that the overall process reduces to only a few key motions during the defining moments of chemistry (i.e., during nuclear passage over a barrier separating one stable structure from another). There is an enormous reduction in dimensionality at the very transition state or critical point in a reaction coordinate, with a corresponding reduction in complexity in terms of looking for general trends.

The fundamental problem underlying this apparent conundrum is that we really only have well-defined structures, and corresponding modes to describe the nuclear fluctuations, at stable minima. The very act of barrier crossing is a rare event involving far-from-equilibrium motions. At these points, the potential energy surface no longer corresponds to the harmonic approximations used to define the vibrational modes and associated motions for a given molecular structure. There are extremely strong curvatures or gradients in the potential energy surface that strongly mix the various degrees of freedom in this region. To get some feel for the forces leading to mode mixing in barrier crossing regions, let us consider the typical potential energy surface shown in **Figure 1**. At the minimum describing the stable, long-lived, structures of the reactants, the surface can be well characterized by a harmonic potential and the different degrees of freedom for the nuclear motions described by an orthonormal set of vibrational eigenfunctions. If one considers a ball rolling on such a surface to represent the effective mass for a given heavy mode, there would only be one frequency of motion uniquely defining each eigenmode. However, let us now consider a ball moving further along this potential. The ball's motion would not be defined by a single frequency or Fourier component but would have to include lower frequencies as the ball experiences different gradients (which correspond to these curvatures). This simple depiction of anharmonic motions shows how the various nuclear degrees of freedom become strongly mixed at saddle points in the many-body potential defining the system. When a spatially extended low-frequency mode is mixed with a high-frequency mode and vibrational overtones, there is a great deal of localization of the largest root mean square (rms) atomic motions (27–29). It is this effect that ultimately leads to localized changes in structure that we call chemistry.

There is still a conceptual problem. This strong mixing between vibrational modes does not change the dimensionality of the problem. We still have as many degrees of freedom, and again the question arises as to how chemical concepts can be transferrable to the degree they are. It is clear the motions become more localized, and it is here that dominant terms in the internuclear potentials are manifest. For example, to construct the potential energy surface for the molecule A-B-C, one needs to include not only terms A-B, B-C, and A-C, but also the three-body term within the potential energy of the corresponding Hamiltonian. More complex systems have higher-order terms. The bonding for the molecule is composed of all these contributing terms. In all cases, the bonding of A to B is dominated by its nearest-neighbor interactions and similarly for bonding B to C. The pairwise terms dominate over higher-order terms within this basis. As the system samples far-from-equilibrium positions on the many-body potential, and the increased rms atomic fluctuations become more localized, the relative strengths of the pair-wise terms become manifest, and one can talk about breaking the weakest bond. It is this feature of reactions that enables

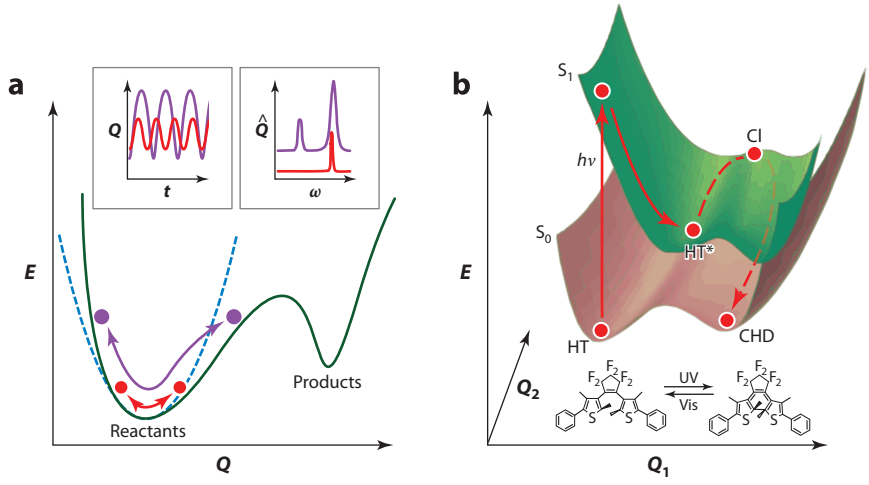

Figure 1

(*a*) Schematic of a simple one-dimensional reaction coordinate, highlighting the differences in motions for an effective mass moving near equilibrium (*red ball* rolling on the potential energy surface) in contrast to the highly anharmonic motions for far-from-equilibrium displacements (*purple ball*). This latter displacement requires the superposition of other frequency components, as seen in the inset, clearly showing the coupling between high- and low-frequency components for such motion. For real systems, the potential energy surface will be much more complex, and the transition probability for passage, as well as the strongly coupled anharmonic motions, needs to be considered. (*b*) Two-dimensional surface (based on 103) illustrating the requirement to optically prepare the system under barrierless conditions to enable the observation of the strongly coupled motions (Q_1, Q_2) for a given reaction coordinate, in this case for the particular ring closing/opening reaction using a reduced molecular structure for diarylethene, the photochemical cycling of which is depicted at the bottom. This surface also shows the effect of a barrier on inferring these relative motions. The stochastic motion in the nearly flat part of the potential (HT* to CI) will be less correlated to the initial state preparation as the system samples the conical intersection (CI) leading ultimately to product formation.

synthetic chemists to use trends within assumed reaction mechanisms to provide an educated guess for constructing a synthetic route.

The time-dependent wave function describing the barrier passage comprises both the electronic and nuclear terms. For reactions occurring along ground state electronic surfaces, the dynamics are generally determined by the nuclear fluctuations, with the electrons adiabatically following this motion. For weakly coupled systems, such as those involved in long-range electron transfer, the reaction occurs nonadiabatically (30). In either case, the changes in the spatial distribution of the electron density during this transition from one electronic surface to another rapidly transform the forces involved, in a highly time-dependent manner. There are currently no simple means to treat the time-dependent structural dynamics and reactive crossing at these points in nuclear configuration space (31). Moreover, these are rare events that must be triggered to have any chance of observing them experimentally. The timescales involved are of the order of a few tens to hundreds of femtoseconds such that femtosecond pump-probe protocols are required to prepare the system on excited state surfaces that access curve-crossing regions between reactant and product surfaces (2). It is precisely at the critical point in curve-crossing regions between excited and ground state surfaces that a breakdown in the Born-Oppenheimer approximation occurs, which leads to the formation of conical intersections between the two surfaces (32–34). At points at which this approximation breaks down, and an avoided crossing forms, the timescale of

the electronic coordinate is rate determining. Theoretical treatments of the reaction dynamics in this region require the highest level of theory, and still electronic correlation effects and other important contributions to the reaction dynamics involve highly simplified approximations to make the problem tractable (31–37). New theoretical methods are clearly needed to help understand the reaction forces in these regions (31, 38). Recent work has been specifically directed to solid state systems to take advantage of the information forthcoming from atomically resolved structural dynamics (39, 40).

In this regard, the new ability to directly resolve far-from-equilibrium motions involved in chemical processes is exciting in that it may soon be possible to experimentally discern trends that help better rationalize and control chemistry. If we can determine classes of localized fluctuations or effective modes for a given reaction type, we can gain control over nuclear passage through the barrier region. More specifically, these projections allow us to determine the structure at the critical point and think about means to control barrier heights and thereby the chemistry. There will undoubtedly be a distribution of structures (such that a free energy representation of the reaction coordinate is more accurate); however, the key modes should be similar for all approaches to the critical region to enable such a reconstruction. This structural information is needed to design methods to emulate biology in terms of controlling barrier heights to direct chemistry. It should be emphasized that the use of reduced dimensionality and propagation of a few key modes involved in reaction dynamics is a well-known strategy in the theoretical community to describe the reaction coordinate (32–34, 37). Some may see this as an oversimplification of the problem, but it turns out, as shown below, that this approach can be experimentally justified. The issue then comes down to the various approximations in properly capturing the key motions and the depiction of the reaction coordinate in the theoretical treatment. There is now a direct experimental method to capture these motions and the reduced dimensionality to rigorously test theory. The partnership between theory and experiment in this pursuit will surely reveal new general trends and change the way we think about chemistry.

3. EXPERIMENTAL CHALLENGES

This section gives an overview of the technical advances that made this class of experiments possible. The work in this area was inspired by initial studies using low-brightness X-ray and electron sources (2, 41–47). The extraordinary constraints imposed by the samples have greatly limited the time resolution and problem selection using low-intensity sources. It was the development of ultrabright electron sources and the means to characterize them that opened up this emerging field of atomically resolved structural dynamics (4). In this respect, the importance of brightness to pursue this class of problems has been equally recognized in the development of X-ray free electron lasers (3, 5, 23). However, only femtosecond time-resolved X-ray absorption/emission experiments on molecular systems have been reported to date (24). Several hard X-ray diffraction studies of structural dynamics of chemical interest are currently in progress.

3.1. Optical State Preparation: Triggering Structural Dynamics

To observe the relative atomic motions directing a structural transition from one stable minimum to another, one must have a means to prepare the system of interest under barrierless conditions (2) (**Figure 1*b***). If there is a barrier involved that is rate limiting, then the observed structural changes will reveal only the initial and intermediate states. Stochastic, uncorrelated, fluctuations in sampling the barrier will wash out the details. As mentioned above, given the timescales involved in barrier crossing, femtosecond optical excitation methods are required for the state preparation.

In this regard, there is a limited number of model systems that can be used to form a basis to develop new chemical concepts. The relevant systems include photoinduced processes such as bond dissociation, photoisomerizations, proton transfer, and ring closing reactions as examples of bond breaking, bond formation, and charge transfer systems. The subsequent motions are followed using pump-probe protocols in which the new feature is that the electron probe pulse is capable of directly resolving atomic motions. Even within this relatively limited basis, there are enough systems to keep physical chemists busy for years, but they do not completely represent the full diversity of chemistry used by synthetic chemists. New methods of initiating chemical reactions under barrierless conditions need to be developed.

In this regard, an important point about this class of experiments needs to be made. The very act of photoinitiating a structural change necessarily modifies the sample such that sample replacement between photoexcitation events is essential. The number of total shots is highly constrained by the finite extent of precious samples. There are also thermal relaxation issues that limit the sampling rate. These may seem like trivial experimental details, but these two conditions put enormous constraints on the brightness of the structural probe. In the most general case, the brightness must be sufficient to give atomic resolution of the structure of interest in a single shot at a given probe delay. Otherwise, one simply runs out of sample before achieving sufficient signal to noise to ascertain the structural changes. It is the finite sample constraints that dictates the requirements for source brightness.

3.2. Development of Ultrabright Electron Sources for Atomically Resolved Dynamics

At the outset, there were three major technological challenges with respect to using electrons to probe structural dynamics of chemical interest with the prerequisite subpicosecond time resolution and brightness to capture atomic motions. Here, I note that the highest structural resolution per scattering event is attained with diffraction or reciprocal space imaging. The source brightness requirements are several orders of magnitude less than real-space imaging, largely because one samples many orders of magnitude more identically prepared systems in diffraction. This review thus focuses on femtosecond electron diffraction. In this regard, the main questions of feasibility were the following:

1. How do we generate electron pulses of >10 A/cm^2 peak current density on target with sufficient spatial coherence (>1 nm) to enable near-single-shot atomically resolved structures (with regard to finite sample constraints)?
2. How do we fully characterize the electron probe pulses to determine the true time resolution at the sample position (with <100-μm accuracy) and sub-100-fs time resolution?
3. How do we determine the $t = 0$ position between the laser excitation and electron probe pulse to synchronize the movie to correlate the temporal response and attain the highest possible time resolution to the structural dynamics?
4. Moreover, most chemistry occurs in the solution phase. We can issue a fourth technical challenge. How can one ever obtain stable liquid flow with path lengths of the order of 100 nm, as required for electron transmission, to probe solution phase chemistry? The liquid phase is generally thought to be the unique domain of femtosecond X-ray scattering.

The first condition is dictated by the degree of excitation needed ($\sim$10% of the lattice) to get above background. At this excitation level, as discussed above, most systems are not fully reversible back to their original state. Either there are irreversible side reactions, or there is crystal damage that accumulates. This peak current density estimate is based on the requirement of approximately

10^4 electrons to obtain sufficient detected diffracted electrons on the relevant 100-fs timescale to secure a dynamic range of at least 100 within limited sample constraints. At this electron density, there are significant electron-electron repulsion or space charge effects that will lead to pulse broadening and loss of spatial coherence; both effects reduce the source brightness. In principle, it is possible to avoid space charge broadening effects on the electron pulse properties by going to very low electron densities, and in the ultimate limit, one could adopt statistically only one electron per pulse to completely avoid space charge broadening effects (48). This approach limits the range of possible studies to systems capable of rapid sample exchange, such as studies of gas phase systems using molecular beam methods or simple reversible (heating) effects (49), which need to be clearly distinguished from net structural transitions or chemical processes. Gas phase samples are currently limited in time resolution to several picoseconds by velocity mismatch between the optical and electron pulses (vide infra). With respect to reversible systems, there are no chemically relevant systems reported to date that are capable of the degree of photon cycling (10^7–10^8) required to statistically be in the single-electron limit with sufficient dynamic range. The technical difficulty is achieving, simultaneously, space-time resolution in the 100-fs and subangstrom domains to capture the primary atomic motions directing chemistry. There are important problems extending over different space-time domains (see 49 for examples of the achieved simultaneous space-time resolution). Another important consideration is that the incident excitation should not exceed 100 GW/cm^2 to avoid multiphoton ionization artifacts and multiple reaction pathways from upper excited states (50–52). The thicker the sample is, the higher is the incident peak power needed to achieve the same degree of lattice excitation. This optical damage threshold and complication in state preparation impose severe constraints on sample thickness such that there are not many differences in sample requirements for either X-ray or electron diffraction. Multiphoton ionization effects are particularly a problem for surface studies, especially in reflection geometries, in which surface charge accumulates in the surface region probed (53–55). In all cases, multiphoton ionization creates electrostatic fields that change the physics of the structural changes, which needs to be avoided.

Sample limitations are the most difficult aspects of this class of experiments. To put it succinctly, one needs approximately 100-fold more samples than for typical crystallography experiments, and the sample thickness must be of the order of a few micrometers or less. These requirements should give some calibration to the importance of source brightness. In all applications, it is better to use the brightest electron or X-ray source possible.

The above experimental challenges give some impression of the obstacles that had to be overcome, primarily due to sample constraints. As discussed below, all the above listed technical challenges have been solved.

3.2.1. Nonrelativistic electrons. The key turning point in source development came from an effectively exact numerical solution to electron pulse propagation at the targeted bunch density for near-single-shot structure conditions (56). **Figure 2*a*** shows the main results that provided the epiphany moment for solving the long-standing space charge problems in electron source brightness. The rapid evolution in the electron pulse parameters at relatively high bunch density is evident. There are two solutions that are immediately apparent. One solution is to make the electron gun as compact as possible (**Figure 2*b***). The other is to deliberately exploit the remarkable linear chirp that naturally develops with nonrelativistic electrons. This calculation showed that it was possible to generate near-perfect linear chirp without significant loss in transverse coherence or spatial resolving power—at the critical electron densities needed for single-shot structure determination. As pointed out in Reference 56, a linear chirp is the simplest time-dependent spatial correlation to invert for pulse compression. One can even further increase the charge density

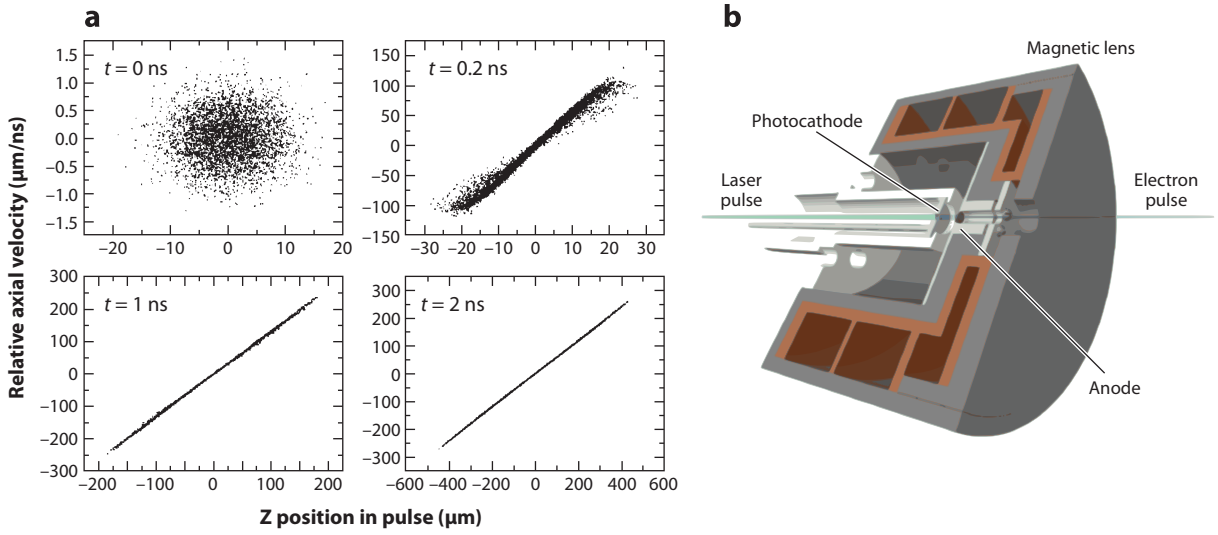

Figure 2

(*a*) Results from an effectively exact solution to the coupled motions of 10,000 electrons, sufficient for single-shot structure determination for systems with unit cells of a few nanometers. The initial electron pulse ($t = 0$ position) replicates the femtosecond laser pulse used for photoinjection and then rapidly evolves owing to electron-electron repulsion or space charge effects. The key point is that the space-time correlation is conserved even for this high bunch charge with minimal effects on the transverse spatial coherence. There are two solutions to high-brightness electron pulses apparent from this calculation: compact electron guns and the use of linear dispersion elements of the opposite sign to compress the pulse at the sample position. Panel *a* taken from Reference 56. (*b*) Schematic illustration of a compact electron gun design that accommodates 1-cm electron propagation path lengths to realize conditions of the top right frame ($t = 0.2$ ns) in panel *a*. Current versions of compact electron guns are capable of 10^5 electrons in a 100-fs to 200-fs pulse (100-μm beam radius) with spatial resolving power sufficient to study the dynamics of unit cells >5 nm.

upon compression by using longer (picosecond) optimized excitation pulses for the photoinjection. This work helped stimulate a large body of theoretical studies on electron source coherence and experimental studies that have borne out these findings (57–64). There are now very accurate numerical and analytical theories for calculating the electron pulse propagation dynamics, as well as experimental methods for full characterization of the electron pulses and $t = 0$ position. This development was essential to advancing electron source brightness.

The first three technical challenges have been met. Based on theoretical modeling, it was possible to come to a good compromise in electron pulse parameters to open up atomically resolved structural dynamics in the critical 100-fs to 1-ps time window to directly observe atomic motions. In fact, the first machines to break the picosecond barrier used compact electron gun designs. This concept is now capable of 200-fs instrument response functions, with up to 10^9 electrons/cm^2, on target with sufficient transverse coherence to study unit cells up to 6 nm. This instrument concept can be advanced by at least another order of magnitude in brightness with improvements in photocathodes (65) and is currently still on par with other source concepts with respect to resolving structural dynamics for small unit cells (<6 nm).

The next major advance in electron gun design exploited the linear chip to compress the pulses. There are several possible electron optical systems that could compensate this chirp (62, 66–69). A particularly elegant solution for high brightness, based on the findings of Reference 56, was developed by the Luiten group (62) using a radiofrequency (RF) cavity to compress the pulse. This work is similar in concept to Reference 68, except that the system was designed for high–bunch charge parameters. In principle, RF pulse compression enables an increase in the

electron bunch density by nearly a factor of 100 over the compact gun design. However, phase jitter between the RF and the excitation pulse used to trigger the structural dynamics has limited the instrument response time to a few hundred femtoseconds (70–72), so the effective increase in brightness is approximately a factor of 10 over compact gun designs. Based on this work, an RF pulse compression system has been developed at the University of Toronto with a magnetic lens system to provide the needed spatial coherence at the sample position and spatial point spread function at the detector plane. The electron pulse propagation dynamics and phase jitter for this system have been fully characterized (71). The capabilities to fully characterize the electron pulse were essential in this regard and ultimately led to the first atomically resolved dynamics with 100-fs time resolution utilizing this concept (22, 73). The time resolution has been further advanced through the use of a zero-jitter photoswitched streak camera for time stamping and correcting the RF jitter to 30 fs (74). This electron source concept is now capable of capturing even the fastest nuclear motions with single-shot capabilities.

The electron source brightness is determined by the source emittance, which determines the transverse momentum spread in the electron distribution at the sample position. The smaller the source size, the smaller is the angular spread at the sample, and the more coherent the source will appear. The challenge is to get as many electrons as possible in a beam with the lowest possible divergence. This condition defines the source brightness, as for any imaging application. The lowest transverse energy spread, or emittance, is achieved near the threshold for photoemission, but this also gives the lowest quantum yield for photoemission, or lower electron intensity. What are the fundamental limits to electron source brightness? This question has been addressed using threshold photoionization of Rydberg states of ultracold atoms to serve as a highly coherent electron source (75–80). This work has pointed out the fundamental limits to source brightness for nonrelativistic electron regimes. As bright as the electron sources are now, it should be possible to further increase the electron source brightness by at least two orders of magnitude.

3.2.2. Relativistic electrons. The high-energy physics community has a long history in developing low-emittance electron sources for applications in particle physics and X-ray generation (81). However, the potential for using electrons for directly studying structural dynamics was not appreciated until femtosecond electron diffraction studies of strongly driven phase transitions (1) demonstrated the importance of high–bunch charge electron pulses to overcome sample limitations. The relativistic electron gun designs typically employ RF cavities to generate extraction fields that are an order of magnitude larger and correspondingly brighter sources than that possible with DC extraction fields used for the current generation of nonrelativistic electron guns.

Hastings et al. (82) were the first to demonstrate a relativistic electron source for possible application in femtosecond diffraction studies. They showed a static diffraction pattern of polycrystalline Al obtained with a single subpicosecond electron pulse (2.9 pC, 5.4 MeV). Musumeci et al. (83) followed this work with a 3.5-MeV source to show single-shot capabilities. The time resolution was limited to 800 fs by RF timing jitter that can be improved by using deflecting cavities or with time-stamping methods (84–86). Tanimura and coworkers (87) introduced a projector lens system similar to that used in commercial transmission electron microscopy (TEM) for diffraction mode imaging. The quality of the diffraction pattern is dramatically improved, with time resolution estimated to be of the order of 100 fs.

The above sources do not take full advantage of the reduced longitudinal space charge broadening within the relativistic regime (all electrons travel near c). The residual chirp imposed by the RF acceleration needs to be compensated to reach the ultimate brightness. The Relativistic Electron Gun for Atomic Exploration (REGAE) developed in Hamburg in collaboration with DESY includes an RF rebunching cavity as a key design concept that compresses the electron pulses down

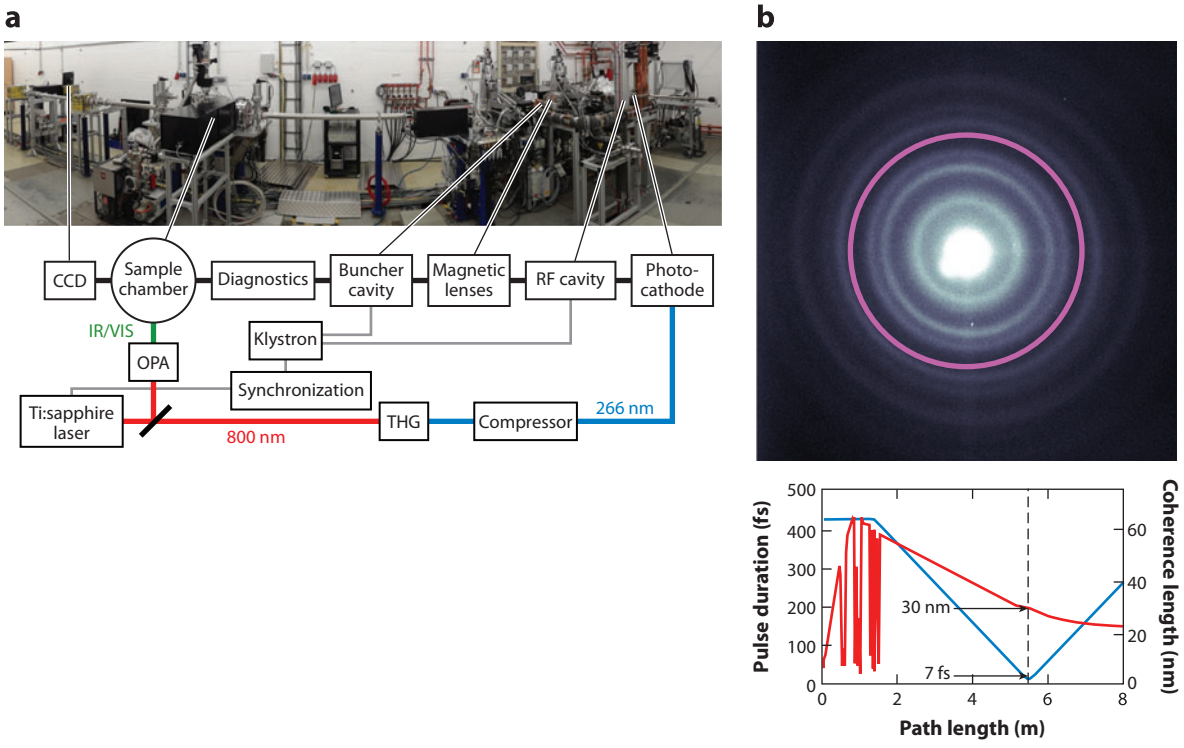

Figure 3

(*a*) Photograph of the Relativistic Electron Gun for Atomic Exploration (REGAE) with a schematic illustration of operational components. For scale, the distance from the radiofrequency cavity/photocathode to the sample is approximately 4 m. (*b*) One of the first diffraction patterns from REGAE showing diffraction from polycrystalline Au well beyond 1 Å (denoted by the superimposed ring). (*Inset*) The new feature of this relativistic electron gun is the rebunching cavity that is capable of providing up to 10^7 electrons in a pulse as short as 7 fs (rms) at the sample position with a transverse spatial coherence of 30 nm, which is sufficient for protein studies. Inset courtesy of K. Floettman, based on Reference 109. Abbreviations: CCD, charge-coupled device; IR/VIS, infrared/visible; OPA, optical parametric amplifier; RF, radiofrequency; THG, third harmonic generation.

to the 10-fs regime, with transverse coherence (>20 nm) sufficient for protein studies. **Figure 3** shows this system schematically, with the first diffraction patterns obtained during commissioning. This electron source concept presents the ultimate limit to electron bunch density with current photocathodes.

The main attraction of relativistic electron sources is the increased penetration depth for given atomic scattering factors that enables the use of thicker samples, approaching micrometer dimensions. This latter feature puts relativistic sources nearly on par with femtosecond X-ray studies in terms of sample requirements.

4. NEW VISTAS FOR ATOM GAZING: FROM TIME-LAPSE PHOTOGRAPHY TO MOLECULAR MOVIES

This section provides some insight into the types of problems that can now be addressed and the potential impact in chemistry. The first experiments of chemical interest were confined to low-brightness sources and gas phase systems (41, 43–46) for rapid sample exchange. The time

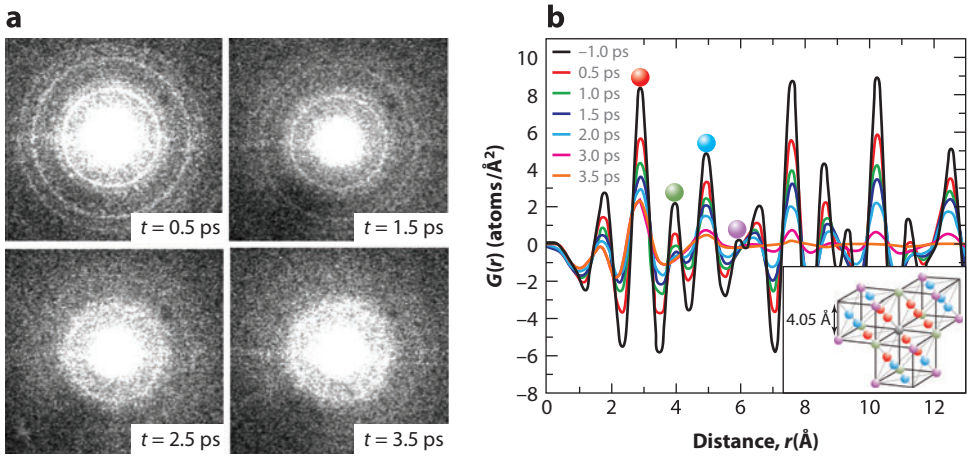

Figure 4

(*a*) Femtosecond electron diffraction studies of strongly driven phase transitions in Al give an atomic view of melting. The rapid lattice collapse is readily observed to occur within 1 ps (from $t = 2.5$ to 3.5 ps) and illustrates that the phase transition involved homogeneous nucleation in which the nucleation size distribution is of the order of 1 nm at this driving force or excitation conditions. (*b*) The reduced density function, $G(r)$, giving the real-space transform of these motions, provides a direct measure of the time-dependent atom-atom pair correlation function on timescales faster than diffusion could blur out the details. The higher diffraction orders decayed on a timescale of a few hundred femtoseconds and required the high time resolution and intensity of this source. Inspection shows that the largest motions involve transverse displacements as part of the onset to the liquid state. Figure taken from Reference 1.

resolution was ultimately limited by velocity mismatch or transit time differences for the electron and light pulses through the sample path length (88). The achieved time-resolution limit was perfect for resolving fully relaxed transient intermediate structures but not for determining the exact pathway through a barrier or curve-crossing region in the excited state surface. There are solutions to this velocity mismatch problem using tilted phase fronts (48), as initially shown in all optical measurements (89, 90). These pioneering gas phase experiments really pointed out the power of time-resolved diffraction experiments and are still considered impressive accomplishments given the very low number density of gas phase molecules.

Figure 4 shows the first experiment with sufficient diffraction orders to fully resolve atomic motions on the prerequisite subpicosecond timescale to catch the primary motions involved in a structural transition, faster than collisional processes could wash out the details (1). The transmission mode for diffraction with thin samples (10–100-nm range) was deliberately used to avoid velocity mismatch limitations to the time resolution. The images shown for polycrystalline Al are similar to the first grainy photographs recorded at the birth of photography. This figure is specifically provided to calibrate the reader to the enormous progress made in electron source brightness over the past 10 years, as discussed below.

These first frames capture the simplest possible structural transition, the act of melting, but under rather special boundary conditions involved in strongly driven phase transitions. This problem dates back to the 1930s, involving a debate concerning the onset of the liquid state (91), which had later ramifications in considering the bound state of matter at extreme pressures and temperatures, as in the interior of planets or stars (92). The ensuing changes in atomic positions following femtosecond laser-induced superheating (heating rates of 10^{15} K/s) can be readily observed even from these grainy first frames without a high level of analysis. At 500 fs, one can see high-order

diffraction rings, illustrating that Al is still in its nascent FCC lattice. At 1.5 ps, these rings become dimmer as the initially excited electrons lose energy to lattice phonons. The increase in rms motion of the atoms reduces the lattice coherence and corresponding diffraction, as described by temperature-dependent Debye-Waller factors. The most astonishing event happens between 2.5 ps and 3.5 ps. There is an incredibly fast lattice collapse in which bonds are broken and the FCC coordination number goes from 12 to an ensemble average of 10 for the unstructured shell-like structure of a liquid. From inspection of the real-space transform, it is possible to watch the lattice literally shake itself apart to form a liquid—at the atomic level. The largest changes involve shear motions with the collapse of the transverse barrier as part of forming the liquid state. Once reaching the critical point for this degree of superheating, the whole melting process occurred within 1 ps. This timescale has to be fully appreciated. This is 10 times faster than this process could occur through normal heterogeneous nucleation. Rather than melting from the surface in an outside-in fashion (heterogeneous nucleation), the system was melting from the inside out. This was the first atomic view of the long-predicted process of homogeneous nucleation that could be used to test the accuracy of atomistic molecular dynamics calculations for this process (93). The melting process was literally occurring faster than the speed of sound and experimentally resolved this old debate.

Most importantly, the fact that the system collapsed to the liquid structure on a 1-ps timescale has great consequences in understanding nucleation growth under strongly driven conditions. This timescale showed that the nucleation sites could only be on average approximately 1 nm in size, involving as few as 10 atoms. This single detail showed how to control nucleation growth and avoid cavitation-induced shock waves and thermal damage in laser-driven ablation. Based on this new insight, it was recognized that shock wave–induced damage in laser surgery could finally be overcome. A picosecond infrared laser tuned to the OH stretch of water in tissue was specifically developed for laser surgery, taking the above new insight into account to provide the correct temporal profile to restrict nucleation growth. The ablation process ejects entire proteins into the gas phase faster than even the collision exchange of the excited water with the protein (94, 95). This is the first method capable of cutting tissue without scar tissue formation (96). The promise of the laser for achieving the fundamental (cellular) limit to minimally invasive surgery has now been achieved (97). This development highlights the importance of this field as even the first atomically resolved structural transition has already had a significant impact that could well transform the quality of medical intervention. Generally, it is difficult to trace the thread from basic science to societal benefits. Here the connection is clear.

Subsequent work in the area has focused for the most part on photoinduced phase transitions. These include strongly driven phase transitions involved in nonthermal melting, the creation of states of warm dense matter, and relatively weak perturbations of strongly correlated electron-lattice systems that give rise to interesting collective phenomena (4). As a representative example of this latter class of experiments, the photoinduced structural phase transition of TaS_2, and the modulation of the charge density wave, provides a particularly good example of the improvement in source brightness and methodology (see **Video 1**). The surprise in viewing this structural change at the space-time limit was that the photoinduced suppression of the charge density wave (200 fs) and its reformation (picoseconds) occurred at the speed limit and clearly illustrated the very strong electron-lattice correlation energy involved in directing this highly cooperative many-body effect (98). This work has been extended to the study of charge density waves in $TaSe_2$, with improved quality in diffraction using a zero-jitter streak camera for movie-mode data collection (99, 100). Subsequent studies of other two-dimensional layered materials within the general class of strongly correlated electron-lattice systems have revealed a wealth of information on the underlying forces leading to structural phase transitions and material properties (101). This general approach could well provide the defining information needed to understand a host of many-body

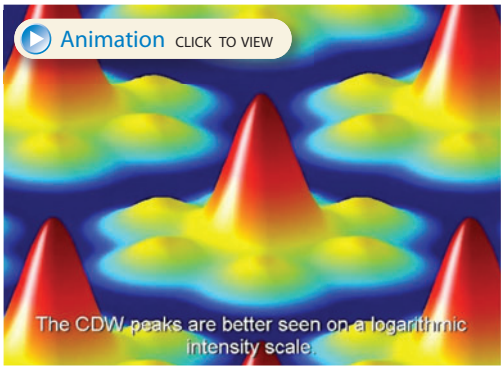

Video 1

Observation of electron correlation effects and cooperative many-body effects in the formation of charge density waves in TaS_2 (98). To view the video, access this article on the Annual Reviews website at **http://www.annualreviews.org**.

problems, from colossal magnetoresistance to high-temperature superconductivity, in that it gives a direct measurement of the electron-lattice coupling over the relevant timescales and length scale.

From a chemistry standpoint, the real power of high-brightness electron sources has been recently demonstrated in the study of the photoinduced structural changes in the interesting organic system EDO-TTF, which can be photoswitched from insulating to metallic properties (22). The photoinduced structural change is formally a photoinduced charge transfer process strongly coupled to nuclear modes stabilizing the change in charge distribution (**Figure 5**). One of the major experimental challenges for electron probes is to increase the brightness to enable the study of weakly scattering organic systems that involve more complex structures and much lower thermal conductivity than previously studied metallic and layered solid state systems. This work was the first to use the RF pulse compression schemes to open up this class of study. To avoid thermal accumulation effects, the experiment had to be conducted at a sampling rate or laser repetition rate of 10 Hz. By direct comparison to higher data-acquisition rates, it was demonstrated that this study would not have been possible without the increased electron source brightness. The quality of the resultant diffraction needs to be fully appreciated (compare the images in **Figure 5** to those in **Figure 4** to see the dramatic improvement in source brightness). There were hundreds of diffraction orders that went out to better than 0.4 Å to serve as constraints in the inversion to time-dependent structures (e.g., see figure 2 and supporting online material of Reference 22 in which the time slices from just a few diffraction orders are shown). The signal-to-noise ratio is comparable to high-quality, integrated all-optical pump-probe measurements, but with a direct connection to structure.

The key new insights to come from this atomic-level view of the photoinduced charge transfer process are shown in **Figure 5*c*,*d***. In comparing the initial and final static structures for the two phases of EDO-TTF, one would expect the bending mode of the EDO moiety to be the dominant mode in sampling the barrier. This motion leads to greater π-π overlap and electron delocalization in forming conduction bands associated with the metallic state. Although this mode is involved, there is again a surprise that leaps out at you only when it is possible to see the structural transition at this atomic level of detail. All reasonable combinations of different modes that connected the two structural end points were explored through a Pearson correlation analysis. The structural changes involved only the nearest neighbors in the lattice, based on the correlation analysis and degree of lattice excitation (measured directly). This highly localized relaxation process is similar

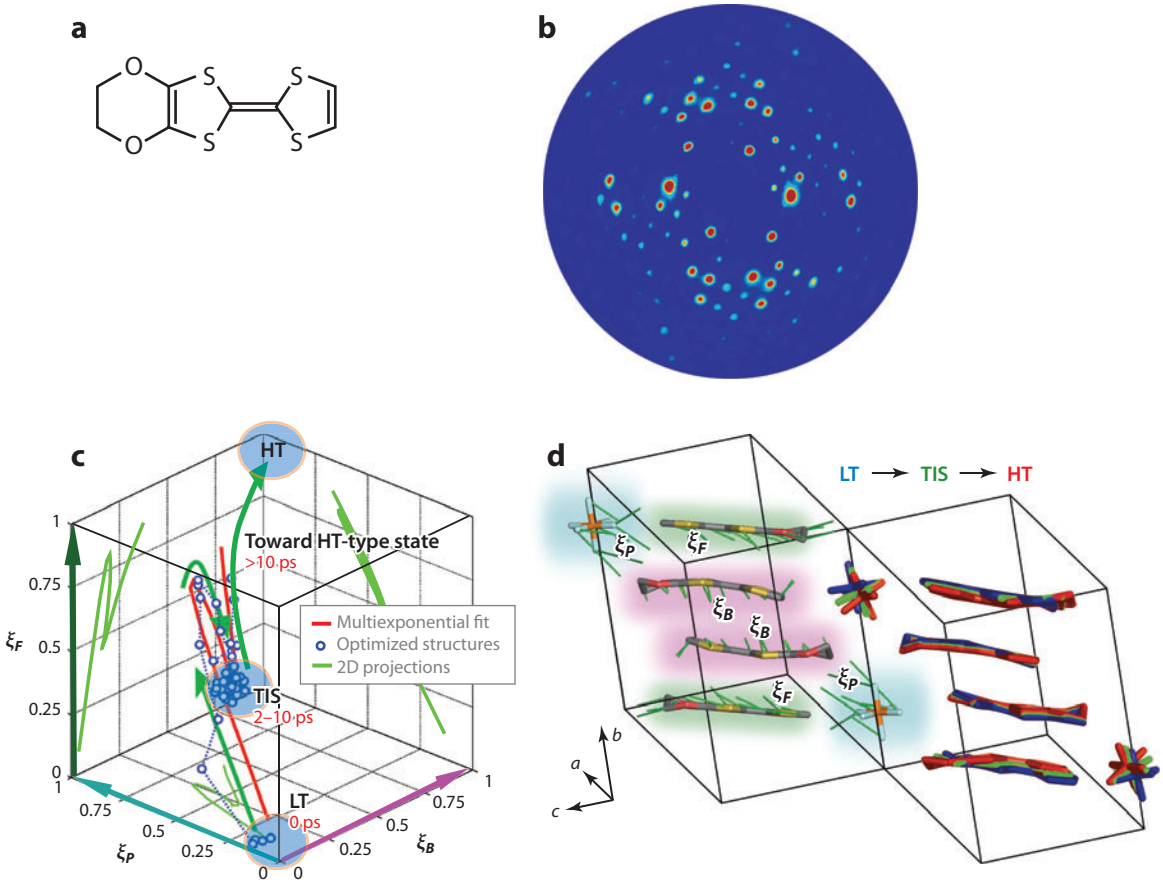

Figure 5

(*a*) Molecular structure of EDO-TTF, as the molecular framework of the $(EDO\text{-}TTF)_2PF_6$ charge ordered system. (*b*) Representative diffraction pattern to illustrate the high quality of diffraction, now possible out to better than 0.4 Å (compare these images to those shown in **Figure 4** to see the dramatic improvement in electron sources). (*c*) Three-dimensional reconstruction of the motion along the three strongly coupled modes that constitute the structural changes accompanying photoinduced charge transfer. These displacements are highly correlated and lead the system from the nascent low-temperature (LT) structure to the new structure corresponding to that of the higher-temperature (HT) form if the system was thermally propagated. The formation of the transient intermediate state (TIS) bridges the two surfaces. (*d*) Schematic depiction of the three strongly coupled modes, ξ_P (motion of the PF_6^- counterion), ξ_B (ring bending coordinate), and ξ_F (sliding motion of the rings), with the direction of motion going from the LT to TIS to HT structures shown by arrows and superposed structures for some sense of animation (see **Video 2** based on the analysis of the dynamic diffraction patterns to gain an atomic perspective on how these strongly coupled modes direct the passage from one structure to another). Figure adapted from Reference 22.

to solvation. All the diffraction orders could be fit by the simple displacement of just three modes: One was the bending coordinate, but there were two others, a sliding motion of the ring center of mass and, most important, the motion of the heavy PF_6^- counterion. This latter motion was not expected. In hindsight, this observation can be readily justified. If one considers the local field created by the photoinduced change in charge distribution, there will be a change in local electric field that will create a force on the counterion. However, there was an even greater surprise in store. Close inspection of the different trajectories along the reaction coordinates in **Figure 5*c*** shows that the motions are strongly coupled. The different trajectories appear as shadow projections on the other two nominally orthogonal coordinates. The motion along these coordinates could have

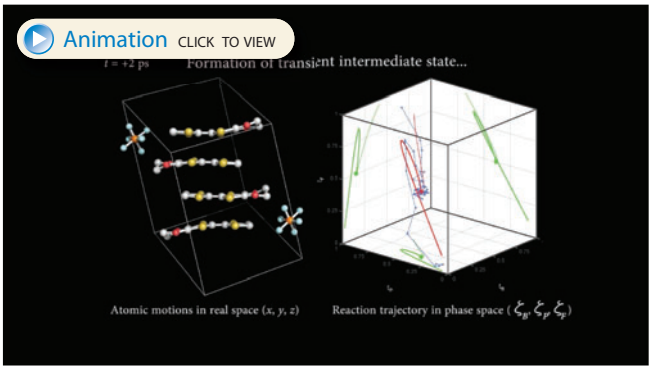

Video 2

Direct observation of the reduction in dimensionality during photoinduced charge transfer for the model organic system EDO-TTF (22). To view the video, access this article on the Annual Reviews website at **http://www.annualreviews.org**.

been anything, but they are obviously very highly correlated (see **Video 2** to fully appreciate the strong coupling of these motions).

This high degree of correlation means that the slowest mode is dominating the overall motion along the reaction coordinate and slaving the net rms displacements along the higher-frequency modes by virtue of its induced change in the many-body potential. The slowest mode in this case is the motion along the PF_6^- coordinate. This is a very large ion, and as it moves, there are clearly steric repulsion terms involved that would lead to a renormalization of the many-body potential. If higher-frequency modes dominate the reaction coordinate, the slowest mode would not be able to track these changes in potential energy surface, and the amplitudes and time course of the displacements would not appear completely correlated as in the present case. Some may have imagined a frozen time slice in the many-body potential that guides the motions through the barrier region or structural transition point, but this line of thinking is out. The importance of the most strongly coupled mode to the reaction coordinate in determining the barrier crossing rates has long been appreciated (6, 7, 32, 33). This motion generally involves a strongly damped low-frequency mode. However, the dynamic coupling between this motion and the other high-frequency modes in reshaping the potential energy surface, and defining the reaction saddle point, was not. It is this effect that leads to the relatively localized atomic motions involved in chemistry. Furthermore, this point is important as it is the projection of the key modes to the reaction saddle point that truly defines the transition state. There will be a large number of nearly degenerate nuclear configurations that lead to structural transitions. Yet these different nuclear configurations must have a high degree of similarity as they would all involve the same key modes in sampling the reaction coordinate, projecting the system over the lowest barrier route. The structural information of the transition state region is needed to develop rational means to control barrier heights. This study now provides the experimental tools to directly observe the key far-from-equilibrium modes to reconstruct these critical points.

The only other study of an organic system that has achieved the necessary space-time resolution to directly observe the correlated atomic motion through barrier crossing regions is that of the photoinduced cyclization–ring opening reaction of diarylethene (52, 73). This study really highlights the importance of using ultrabright electron sources. This system was specifically designed to serve as a photochromic material, capable of undergoing over 10,000 photon cycling processes (102). This system would appear to be a strong candidate for low–electron bunch charge sources or

even single-electron pulse probes. However, this degree of photocycling is only for low fractional excitation. At the approximately 10% lattice excitation needed to observe the structural changes above background, even this system is only capable of approximately 100 photocycles before irreversible changes occur, likely owing to side reactions. Again, the importance of high-brightness electron sources was the key enabling development that allowed these studies.

This system serves as an ideal model for cyclization reactions with conserved stereochemistry. As in the case of EDO-TTF, there is an enormous reduction in the nuclear degrees of freedom coupled to the reaction coordinate. Focusing on the ring closing process, the initial motion is dominated by the bending coordinate around the central bond that involves the whole molecule with a period of 55 cm^{-1} (73). This is the key mode that directs the system to the seam in the reaction coordinate. This displacement brings the two central carbon atoms involved in the ring closing into close proximity. The question is, how does such a spatially delocalized mode lead to the highly localized motions needed to close the ring? Again there is a surprise. Rather than going through what would be considered the classic transition state, which involves a barrier in the excited state surface (see **Figure 1*b***), there are higher-frequency motions that couple the excited state surface to the ground state of the ring closed photoproduct state. This strong vibrational nonadiabatic coupling is difficult to treat theoretically and necessitates the use of truncated model compounds to gain insight into the process (103). The potential shown in **Figure 1*b*** will need to be modified by higher-level treatments. Experimentally, it was possible to cast out a series of localized rotational motions that mix to produce the ring closed form. These displacements occur on a picosecond timescale, involving additional seams connecting the product and ground state from the excited state, such that the degree of correlation or mode coupling as observed in EDO-TTF is not so apparent. The ultrafast nature of this process still clearly separates the possible modes that are involved and highlights the importance of sufficient space-time resolution to connect the initial low-frequency mode to the localized rotational coordinates (see **Video 3** for the atomic motions involved). This atomic-level view of the cyclization process gives remarkable insight into the highly reduced dimensionality of the problem and the key modes involved in terms of directing this process and conserving stereochemistry.

The above examples are for solid state chemistry and are just the beginning. The technology has now advanced to the stage at which the experiments will only be limited by sample issues. It will be important to extend this methodology to the gas and solution phases, for the same

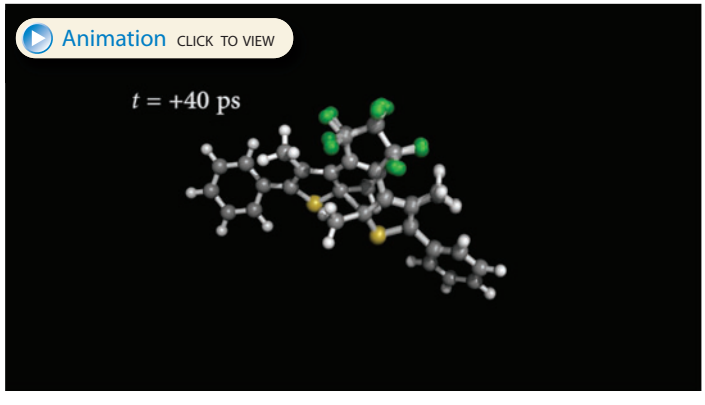

Video 3

Atomically resolved ring closing/bond formation dynamics for diarylethene. To view the video, access this article on the Annual Reviews website at **http://www.annualreviews.org**.

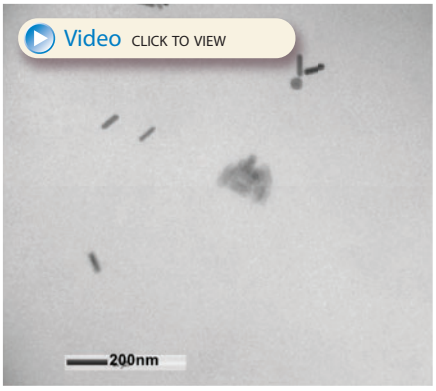

Video 4

Real-space in situ observations of nanoparticle motions in liquid (106). To view the video, access this article on the Annual Reviews website at **http://www.annualreviews.org**.

system, to isolate the effect of the solvent or intermolecular terms on the reaction coordinate. This goal is truly one of the main directives of physical chemistry—to come to an atomic-level understanding of reaction dynamics in the solution phase in which most chemistry and biology occur. Impressive gains have been made in gas phase studies by increasing the information content in the scattering process by using laser alignment (104, 105). The solution phase can be considered to be the most challenging frontier for electron structural probes. This problem has been around since the development of TEM. The technical issue is that in situ liquid studies require liquid path lengths from 50 to 300 nm, depending on the electron energy, ideally with flow within high-vacuum conditions to avoid excessive ambient background electron scattering. The last hurdle to this problem has been recently solved using Si nanofabrication methods in combination with a new concept of dynamic stabilization exploiting negative feedback to damp path-length variations (106). It is now possible to have flow and actively maintain liquid path lengths as short as 45 nm over window areas specifically designed for optical excitation. With this advance, it is now possible to use electrons for real-space imaging within a transmission electron microscope and conserve better than 1-nm spatial resolution (see **Video 4**). This development promises to open up even solution phase chemistry to atomic-level exploration, especially used in conjunction with the latest advances in relativistic and higher energy nonrelativistic electron sources.

One other important area in which the high-scattering cross sections of electron probes have distinct advantages is in the study of surface reaction dynamics and surface reconstruction (107). In this domain, the development of nanoemitters for very high spatial coherence (108) holds great promise in opening up femtosecond low-energy electron diffraction of surface reaction dynamics. These are inherently single- to few-electron sources, so all the problems in dealing with irreversible processes enter the discussion. The most attractive feature of these sources is the high spatial coherence, which may provide details on structural intermediates, not accessible by any other means.

In closing, it is fair to say that the technical challenges posed for the development of electron sources have been met. Essentially all of chemistry can now be studied at the atomic level of inspection over the relevant length scales and timescales. Improvements in source brightness will continue as needed. However, the development of samples that probe different aspects of chemistry is the new frontier, as it should be. The future of atomically resolved structural dynamics is bright indeed.

DISCLOSURE STATEMENT

The author is not aware of any affiliations, memberships, funding, or financial holdings that might be perceived as affecting the objectivity of this review.

ACKNOWLEDGMENTS

The results reported for REGAE are credited to D. Zhang, J. Hirscht, A. Casandruc, S. Bayesteh, M. Hada, S. Manz, H. Delsim-Hashemi, and K. Floettmann. The author was supported by the Natural Sciences and Engineering Research Council of Canada, the Canada Foundation for Innovation, and the Max Planck Society.

LITERATURE CITED

1. Siwick BJ, Dwyer JR, Jordan RE, Miller RJD. 2003. An atomic-level view of melting using femtosecond electron diffraction. *Science* 302:1382–85
2. Dwyer JR, Hebeisen CT, Ernstorfer R, Harb M, Deyirmenjian VB, et al. 2006. Femtosecond electron diffraction: "making the molecular movie." *Philos. Trans. R. Soc. Math. Phys. Eng. Sci.* 364:741–78
3. Bostedt C, Bozek JD, Bucksbaum PH, Coffee RN, Hastings JB, et al. 2013. Ultra-fast and ultra-intense x-ray sciences: first results from the Linac Coherent Light Source free-electron laser. *J. Phys. B* 46:164003
4. Sciaini G, Miller RJD. 2011. Femtosecond electron diffraction: heralding the era of atomically resolved dynamics. *Rep. Prog. Phys.* 74:096101
5. Barty A, Küpper J, Chapman HN. 2013. Molecular imaging using X-ray free-electron lasers. *Annu. Rev. Phys. Chem.* 64:415–35
6. Hänggi P, Borkovec M. 1990. Reaction-rate theory: fifty years after Kramers. *Rev. Mod. Phys.* 62:251–341
7. Schmickler W. 1986. A theory of adiabatic electron-transfer reactions. *J. Electroanal. Chem. Interfacial Electrochem.* 204:31–43
8. Polanyi JC, Zewail AH. 1995. Direct observation of the transition state. *Acc. Chem. Res.* 28:119–32
9. Evans MG, Polanyi M. 1935. Some applications of the transition state method to the calculation of reaction velocities, especially in solution. *Trans. Faraday Soc.* 31:875–94
10. Seno Y, Gō N. 1990. Deoxymyoglobin studied by the conformational normal mode analysis. *J. Mol. Biol.* 216:111–26
11. Genberg L, Richard L, McLendon G, Miller R. 1991. Direct observation of global protein motion in hemoglobin and myoglobin on picosecond time scales. *Science* 251:1051–54
12. Bahar I, Rader A. 2005. Coarse-grained normal mode analysis in structural biology. *Curr. Opin. Struct. Biol.* 15:586–92
13. Kitao A, Go N. 1999. Investigating protein dynamics in collective coordinate space. *Curr. Opin. Struct. Biol.* 9:164–69
14. Lange OF, Grubmüller H. 2007. Full correlation analysis of conformational protein dynamics. *Proteins Struct. Funct. Bioinforma.* 70:1294–312
15. Miller RJD. 1994. Energetics and dynamics of deterministic protein motion. *Acc. Chem. Res.* 27:145–50
16. Maguid S, Fernandez-Alberti S, Echave J. 2008. Evolutionary conservation of protein vibrational dynamics. *Gene* 422:7–13
17. Plusquellic DF, Siegrist K, Heilweil EJ, Esenturk O. 2007. Applications of terahertz spectroscopy in biosystems. *ChemPhysChem* 8:2412–31
18. Sage J, Durbin S, Sturhahn W, Wharton D, Champion P, et al. 2001. Long-range reactive dynamics in myoglobin. *Phys. Rev. Lett.* 86:4966–69
19. Armstrong MR. 2003. Observation of the cascaded atomic-to-global length scales driving protein motion. *Proc. Natl. Acad. Sci. USA* 100:4990–94
20. Goodno GD, Astinov V, Miller RJD. 1999. Femtosecond heterodyne-detected four-wave-mixing studies of deterministic protein motions. 2. Protein response. *J. Phys. Chem. A* 103:10630–43
21. Miller RJD. 2002. 2000 John C. Polanyi Award Lecture: Mother Nature and the molecular Big Bang. *Can. J. Chem.* 80:1–24

22. Gao M, Lu C, Jean-Ruel H, Liu LC, Marx A, et al. 2013. Mapping molecular motions leading to charge delocalization with ultrabright electrons. *Nature* 496:343–46
23. Emma P, Akre R, Arthur J, Bionta R, Bostedt C, et al. 2010. First lasing and operation of an ångstrom-wavelength free-electron laser. *Nat. Photonics* 4:641–47
24. Dell'Angela M, Anniyev T, Beye M, Coffee R, Fohlisch A, et al. 2013. Real-time observation of surface bond breaking with an X-ray laser. *Science* 339:1302–5
25. Freyer B, Zamponi F, Juveé V, Stingl J, Woerner M, et al. 2013. Ultrafast inter-ionic charge transfer of transition-metal complexes mapped by femtosecond X-ray powder diffraction. *J. Chem. Phys.* 138:144504
26. Elsaesser T, Woerner M. 2010. Photoinduced structural dynamics of polar solids studied by femtosecond X-ray diffraction. *Acta Crystallogr. A* 66:168–78
27. Henry BR, Kjaergaard HG. 2002. Local modes. *Can. J. Chem.* 80:1635–42
28. Henry BR, Miller RJD. 1978. Intramolecular perturbation of CH-stretching diagonal local mode anharmonicity in methyl substituted alkanes. *Chem. Phys. Lett.* 60:81–84
29. Jensen P. 2000. An introduction to the theory of local mode vibrations. *Mol. Phys.* 98:1253–85
30. Nielsen S, Kapral R, Ciccotti G. 2000. Mixed quantum-classical surface hopping dynamics. *J. Chem. Phys.* 112:6543–53
31. Abedi A, Agostini F, Suzuki Y, Gross EKU. 2013. Dynamical steps that bridge piecewise adiabatic shapes in the exact time-dependent potential energy surface. *Phys. Rev. Lett.* 110:263001
32. Levine BG, Martínez TJ. 2007. Isomerization through conical intersections. *Annu. Rev. Phys. Chem.* 58:613–34
33. Domcke W, Yarkony DR. 2012. Role of conical intersections in molecular spectroscopy and photoinduced chemical dynamics. *Annu. Rev. Phys. Chem.* 63:325–52
34. Bernardi F, Olivucci M, Robb MA. 1996. Potential energy surface crossings in organic photochemistry. *Chem. Soc. Rev.* 25:321–28
35. Ben-Nun M, Quenneville J, Martínez TJ. 2000. Ab initio multiple spawning: photochemistry from first principles quantum molecular dynamics. *J. Phys. Chem. A* 104:5161–75
36. Nenov A, de Vivie-Riedle R. 2012. Conical intersection seams in polyenes derived from their chemical composition. *J. Chem. Phys.* 137:074101
37. Altoè P, Stenta M, Bottoni A, Garavelli M. 2007. A tunable QM/MM approach to chemical reactivity, structure and physico-chemical properties prediction. *Theor. Chem. Acc.* 118:219–40
38. Ruiz-Barragan S, Robb MA, Blancafort L. 2013. Conical intersection optimization based on a double Newton-Raphson algorithm using composed steps. *J. Chem. Theory Comput.* 9:1433–42
39. Kochman MA, Morrison CA. 2013. Hybrid QM/QM simulations of excited-state intramolecular proton transfer in the molecular crystal 7-(2-pyridyl)-indole. *J. Chem. Theory Comput.* 9:1182–92
40. Kochman MA, Bil A, Morrison CA. 2013. Hybrid QM/QM simulations of photochemical reactions in the molecular crystal *N*-salicylidene-2-chloroaniline. *Phys. Chem. Chem. Phys.* 15:10803–16
41. Ischenko AA, Golubkov VV, Spiridonov VP, Zgurskii AV, Akhmanov AS, et al. 1983. A stroboscopical gas-electron diffraction method for the investigation of short-lived molecular species. *Appl. Phys. B* 32:161–63
42. Williamson S, Mourou G, Li JCM. 1984. Time-resolved laser-induced phase transformation in aluminum. *Phys. Rev. Lett.* 52:2364–67
43. Williamson JC, Dantus M, Kim SB, Zewail AH. 1992. Ultrafast diffraction and molecular structure. *Chem. Phys. Lett.* 196:529–34
44. Williamson JC, Cao J, Ihee H, Frey H, Zewail AH. 1997. Clocking transient chemical changes by ultrafast electron diffraction. *Nature* 386:159–62
45. Dudek RC, Weber PM. 2001. Ultrafast diffraction imaging of the electrocyclic ring-opening reaction of 1,3-cyclohexadiene. *J. Phys. Chem. A* 105:4167–71
46. Ihee H, Lobastov VA, Gomez UM, Goodson BM, Srinivasan R, et al. 2001. Direct imaging of transient molecular structures with ultrafast diffraction. *Science* 291:458–62
47. Chergui M, Zewail AH. 2009. Electron and X-ray methods of ultrafast structural dynamics: advances and applications. *ChemPhysChem* 10:28–43
48. Baum P, Zewail AH. 2006. Breaking resolution limits in ultrafast electron diffraction and microscopy. *Proc. Natl. Acad. Sci. USA* 103:16105–10

49. Flannigan DJ, Zewail AH. 2012. 4D electron microscopy: principles and applications. *Acc. Chem. Res.* 45:1828–39
50. Prokhorenko VI, Halpin A, Johnson PJM, Miller RJD, Brown LS. 2011. Coherent control of the isomerization of retinal in bacteriorhodopsin in the high intensity regime. *J. Chem. Phys.* 134:085105
51. Lincoln CN, Fitzpatrick AE, van Thor JJ. 2012. Photoisomerisation quantum yield and non-linear cross-sections with femtosecond excitation of the photoactive yellow protein. *Phys. Chem. Chem. Phys.* 14:15752
52. Jean-Ruel H. 2013. *Femtosecond electron diffraction studies of molecular reaction dynamics*. PhD Diss., Univ. Toronto
53. Park H, Zuo JM. 2009. Direct measurement of transient electric fields induced by ultrafast pulsed laser irradiation of silicon. *Appl. Phys. Lett.* 94:251103
54. Park H, Zuo J-M. 2010. Comment on "Structural preablation dynamics of graphite observed by ultrafast electron crystallography." *Phys. Rev. Lett.* 105:059603
55. Carbone F, Baum P, Rudolf P, Zewail AH. 2010. Carbone et al. reply. *Phys. Rev. Lett.* 105:059604
56. Siwick BJ, Dwyer JR, Jordan RE, Miller RJD. 2002. Ultrafast electron optics: propagation dynamics of femtosecond electron packets. *J. Appl. Phys.* 92:1643–48
57. Michalik AM, Sipe JE. 2006. Analytic model of electron pulse propagation in ultrafast electron diffraction experiments. *J. Appl. Phys.* 99:054908
58. Michalik AM, Sherman EY, Sipe JE. 2008. Theory of ultrafast electron diffraction: the role of the electron bunch properties. *J. Appl. Phys.* 104:054905
59. Michalik AM, Sipe JE. 2009. Evolution of non-Gaussian electron bunches in ultrafast electron diffraction experiments: comparison to analytic model. *J. Appl. Phys.* 105:084913
60. Reed BW. 2006. Femtosecond electron pulse propagation for ultrafast electron diffraction. *J. Appl. Phys.* 100:034916
61. Gahlmann A, Park ST, Zewail AH. 2008. Ultrashort electron pulses for diffraction, crystallography and microscopy: theoretical and experimental resolutions. *Phys. Chem. Chem. Phys.* 10:2894–909
62. van Oudheusden T, de Jong EF, van der Geer SB, Op 't Root WPEM, Luiten OJ, Siwick BJ. 2007. Electron source concept for single-shot sub-100 fs electron diffraction in the 100 keV range. *J. Appl. Phys.* 102:093501
63. Hebeisen CT, Ernstorfer R, Harb M, Dartigalongue T, Jordan RE, Miller RJD. 2006. Femtosecond electron pulse characterization using laser ponderomotive scattering. *Opt. Lett.* 31:3517–19
64. Hebeisen CT, Sciaini G, Harb M, Ernstorfer R, Dartigalongue T, et al. 2008. Grating enhanced ponderomotive scattering for visualization and full characterization of femtosecond electron pulses. *Opt. Express* 16:3334–41
65. Dowell DH, Bazarov I, Dunham B, Harkay K, Hernandez-Garcia C, et al. 2010. Cathode R&D for future light sources. *Nucl. Instrum. Methods Phys. Res. A* 622:685–97
66. Kassier GH, Haupt K, Erasmus N, Rohwer EG, Schwoerer H. 2009. Achromatic reflectron compressor design for bright pulses in femtosecond electron diffraction. *J. Appl. Phys.* 105:113111
67. Kassier GH, Erasmus N, Haupt K, Boshoff I, Siegmund R, et al. 2012. Photo-triggered pulsed cavity compressor for bright electron bunches in ultrafast electron diffraction. *Appl. Phys. B* 109:249–57
68. Veisz L, Kurkin G, Chernov K, Tarnetsky V, Apolonski A, et al. 2007. Hybrid DC-AC electron gun for fs-electron pulse generation. *New J. Phys.* 9:451–51
69. Tokita S, Hashida M, Inoue S, Nishoji T, Otani K, Sakabe S. 2010. Single-shot femtosecond electron diffraction with laser-accelerated electrons: experimental demonstration of electron pulse compression. *Phys. Rev. Lett.* 105:215004
70. van Oudheusden T, Pasmans PLEM, van der Geer SB, de Loos MJ, van der Wiel MJ, Luiten OJ. 2010. Compression of subrelativistic space-charge-dominated electron bunches for single-shot femtosecond electron diffraction. *Phys. Rev. Lett.* 105:264801
71. Gao M, Jean-Ruel H, Cooney RR, Stampe J, de Jong M, et al. 2012. Full characterization of RF compressed femtosecond electron pulses using ponderomotive scattering. *Opt. Express* 20:12048–58
72. Chatelain RP, Morrison VR, Godbout C, Siwick BJ. 2012. Ultrafast electron diffraction with radio-frequency compressed electron pulses. *Appl. Phys. Lett.* 101:081901

73. Jean-Ruel H, Gao M, Kochman MA, Lu C, Liu LC, et al. 2013. Ring-closing reaction in diarylethene captured by femtosecond electron. *J. Phys. Chem. B* 117:15894–902
74. Gao M, Jiang Y, Kassier GH, Miller RJD. 2013. Single shot time stamping of ultrabright radio frequency compressed electron pulses. *Appl. Phys. Lett.* 103:033503
75. Claessens BJ, van der Geer SB, Taban G, Vredenbregt EJD, Luiten OJ. 2005. Ultracold electron source. *Phys. Rev. Lett.* 95:164801
76. McCulloch AJ, Sheludko DV, Saliba SD, Bell SC, Junker M, et al. 2011. Arbitrarily shaped high-coherence electron bunches from cold atoms. *Nat. Phys.* 7:785–88
77. Debernardi N, van Vliembergen RWL, Engelen WJ, Hermans KHM, Reijnders MP, et al. 2012. Optimization of the current extracted from an ultracold ion source. *New J. Phys.* 14:083011
78. Saliba SD, Putkunz CT, Sheludko DV, McCulloch AJ, Nugent KA, Scholten RE. 2012. Spatial coherence of electron bunches extracted from an arbitrarily shaped cold atom electron source. *Opt. Express* 20:3967–74
79. Taban G, Reijnders MP, Fleskens B, van der Geer SB, Luiten OJ, Vredenbregt EJD. 2010. Ultracold electron source for single-shot diffraction studies. *Eur. Phys. Lett.* 91:46004
80. Engelen WJ, van der Heijden MA, Bakker DJ, Vredenbregt EJD, Luiten OJ. 2013. High-coherence electron bunches produced by femtosecond photoionization. *Nat. Commun.* 4:1693
81. Travier C. 1991. RF guns: bright injectors for FEL. *Nucl. Instrum. Methods Phys. Res. A* 304:285–96
82. Hastings JB, Rudakov FM, Dowell DH, Schmerge JF, Cardoza JD, et al. 2006. Ultrafast time-resolved electron diffraction with megavolt electron beams. *Appl. Phys. Lett.* 89:184109
83. Musumeci P, Moody JT, Scoby CM, Gutierrez MS, Westfall M. 2010. Laser-induced melting of a single crystal gold sample by time-resolved ultrafast relativistic electron diffraction. *Appl. Phys. Lett.* 97:063502
84. Li R, Huang W, Du Y, Yan L, Du Q, et al. 2010. Note: single-shot continuously time-resolved MeV ultrafast electron diffraction. *Rev. Sci. Instrum.* 81:036110
85. Musumeci P, Moody JT, Scoby CM, Gutierrez MS, Westfall M, Li RK. 2010. Capturing ultrafast structural evolutions with a single pulse of MeV electrons: radio frequency streak camera based electron diffraction. *J. Appl. Phys.* 108:114513
86. Scoby CM, Musumeci P, Moody JT, Gutierrez MS. 2010. Electro-optic sampling at 90 degree interaction geometry for time-of-arrival stamping of ultrafast relativistic electron diffraction. *Phys. Rev. Spec. Top. Accel. Beams* 13:022801
87. Murooka Y, Naruse N, Sakakihara S, Ishimaru M, Yang J, Tanimura K. 2011. Transmission-electron diffraction by MeV electron pulses. *Appl. Phys. Lett.* 98:251903
88. Williamson JC, Zewail AH. 1993. Ultrafast electron diffraction: velocity mismatch and temporal resolution in crossed-beam experiments. *Chem. Phys. Lett.* 209:10–16
89. Goodno GD, Astinov V, Miller RJD. 1999. Diffractive optics-based heterodyne-detected grating spectroscopy: application to ultrafast protein dynamics. *J. Phys. Chem. B* 103:603–7
90. Maznev AA, Crimmins TF, Nelson KA. 1998. How to make femtosecond pulses overlap. *Opt. Lett.* 23:1378–80
91. Born M. 1939. Thermodynamics of crystals and melting. *J. Chem. Phys.* 7:591–603
92. Ernstorfer R, Harb M, Hebeisen CT, Sciaini G, Dartigalongue T, Miller RJD. 2009. The formation of warm dense matter: experimental evidence for electronic bond hardening in gold. *Science* 323:1033–37
93. Lin Z, Zhigilei L. 2006. Time-resolved diffraction profiles and atomic dynamics in short-pulse laser-induced structural transformations: molecular dynamics study. *Phys. Rev. B* 73:184113
94. Franjic K, Cowan ML, Kraemer D, Miller RJD. 2009. Laser selective cutting of biological tissues by impulsive heat deposition through ultrafast vibrational excitations. *Opt. Express* 17:22937–59
95. Franjic K, Miller RJD. 2010. Vibrationally excited ultrafast thermodynamic phase transitions at the water/air interface. *Phys. Chem. Chem. Phys.* 12:5225–39
96. Amini-Nik S, Kraemer D, Cowan ML, Gunaratne K, Nadesan P, et al. 2010. Ultrafast mid-IR laser scalpel: protein signals of the fundamental limits to minimally invasive surgery. *PLoS One* 5:e13053
97. Hess M, Hildebrandt MD, Müller F, Kruber S, Kroetz P, et al. 2013. Picosecond infrared laser (PIRL): an ideal phonomicrosurgical laser? *Eur. Arch. Otorhinolaryngol.* 270:2927–37
98. Eichberger M, Schaefer H, Krumova M, Beyer M, Demsar J, et al. 2010. Snapshots of cooperative atomic motions in the optical suppression of charge density waves. *Nature* 468:799–802

99. Erasmus N, Eichberger M, Haupt K, Boshoff I, Kassier G, et al. 2012. Ultrafast dynamics of charge density waves in $4H_b$-$TaSe_2$ probed by femtosecond electron diffraction. *Phys. Rev. Lett.* 109:167402
100. Eichberger M, Erasmus N, Haupt K, Kassier G, von Flotow A, et al. 2013. Femtosecond streaking of electron diffraction patterns to study structural dynamics in crystalline matter. *Appl. Phys. Lett.* 102:121106
101. Han T-RT, Tao Z, Mahanti SD, Chang K, Ruan C-Y, et al. 2012. Structural dynamics of two-dimensional charge-density waves in $CeTe_3$ investigated by ultrafast electron crystallography. *Phys. Rev. B* 86:075145
102. Irie M. 2001. Reversible surface morphology changes of a photochromic diarylethene single crystal by photoirradiation. *Science* 291:1769–72
103. Boggio-Pasqua M, Ravaglia M, Bearpark MJ, Garavelli M, Robb MA. 2003. Can diarylethene photochromism be explained by a reaction path alone? A CASSCF study with model MMVB dynamics. *J. Phys. Chem. A* 107:11139–52
104. Reckenthaeler P, Centurion M, Fuß W, Trushin SA, Krausz F, Fill EE. 2009. Time-resolved electron diffraction from selectively aligned molecules. *Phys. Rev. Lett.* 102:213001
105. Hensley CJ, Yang J, Centurion M. 2012. Imaging of isolated molecules with ultrafast electron pulses. *Phys. Rev. Lett.* 109:133202
106. Mueller C, Harb M, Dwyer JR, Miller RJD. 2013. Nanofluidic cells with controlled pathlength and liquid flow for rapid, high-resolution in situ imaging with electrons. *J. Phys. Chem. Lett.* 4:2339–47
107. Hanisch-Blicharski A, Janzen A, Krenzer B, Wall S, Klasing F, et al. 2013. Ultra-fast electron diffraction at surfaces: from nanoscale heat transport to driven phase transitions. *Ultramicroscopy* 127:2–8
108. Paarmann A, Gulde M, Müller M, Schäfer S, Schweda S, et al. 2012. Coherent femtosecond low-energy single-electron pulses for time-resolved diffraction and imaging: a numerical study. *J. Appl. Phys.* 112:113109
109. Floettman K. 2013. Generation of sub-fs electron beams at few-MeV energies. *Nucl. Instrum. Methods Phys. Res. A.* In press